arXiv:cond-mat/0403136v1 [cond-mat.supr-con] 4 Mar 2004

The Electronic and Superconducting Properties of Oxygen-Ordered MgB_2 compounds of the form $Mg_2B_3O_x$

Juan C. Idrobo
*Department of Physics, University of California-Davis, Davis, One Shields Ave, Davis CA, 95616, USA**

Serdar Öğüt
Department of Physics, University of Illinois at Chicago, 845 West Taylor Street (M/C 273), Chicago, IL 60607

Taner Yildirim
NIST Center for Neutron Research, National Institute of Standards and Technology, Gaithersburg, Maryland 20899 USA

Robert F. Klie
Brookhaven National Laboratory, Upton, New York 11973

Nigel D. Browning
Dept. of Chemical Engineering and Material Science, University of California-Davis, One Shields Ave, Davis CA, 95616, USA and National Center for Electron Microscopy, Lawrence Berkeley National Laboratory, Berkeley, CA 94720 USA

(Dated: February 2, 2008)

Possible candidates for the $Mg_2B_3O_x$ nanostructures observed in bulk of polycrystalline MgB_2 [1] have been studied using a combination of Z-contrast imaging, electron energy loss spectroscopy (EELS) and first-principles calculations. The electronic structures, phonon modes, and electron phonon coupling parameters are calculated for two oxygen-ordered MgB_2 compounds of composition Mg_2B_3O and $Mg_2B_3O_2$, and compared with those of MgB_2. We find that the density of states for both $Mg_2B_3O_x$ structures show very good agreement with EELS, indicating that they are excellent candidates to explain the observed coherent oxygen precipitates. Incorporation of oxygen reduces the transition temperature and gives calculated T_C values of 18.3 K and 1.6 K for Mg_2B_3O and $Mg_2B_3O_2$, respectively.

The discovery of superconductivity in MgB_2 with a transition temperature of 40 K [2] has attracted the attention of the scientific community for two main reasons: the technological applications of this material and the new insights that such a simple structure could bring to superconductivity theory. Efforts to improve the superconductivity properties of MgB_2 have included doping with elements such as Y [3], Zr [4], C [5], Al [6], Cu and Ag [7], but the results varied for different groups. A simple explanation for this behavior is that the transport properties of MgB_2 have a strong dependence on the sample preparation conditions, which makes it hard to obtain unambiguous results even for undoped samples [8]. In fact, there have been reports from different groups showing that MgB_2 samples are not a single phase material, but rather a rich collection of different phases including MgB_2, MgO, B_yO_x, Mg_xB_y, $Mg_xB_yO_z$ [1, 9, 10, 11]. Oxygen, unlike some other elements, is present in MgB_2 as an unintentional impurity due to its high reactivity with MgB_2. Typically, oxygen rich precipitates form in the bulk of MgB_2 where they contribute to the overall transport properties through flux pinning [11]. Moreover, oxygen can segregate at grain boundaries of MgB_2 where, unlike the high$-T_c$ materials, it contributes significantly to flux pinning, increasing the overall J_C as the grain size decreases [12]. MgB_2 has already been used in making wires [13], tapes [14], and Josephson junctions [15], and in order to improve the properties of such devices, the effect that oxygen has on the properties of MgB_2 needs to be well understood. Surprisingly, the importance of oxygen in the development of MgB_2 devices has been overlooked, and detailed first-principles studies of oxygen ordering and segregation have not yet been performed.

It was previously reported that oxygen impurities can increase the upper critical fields and critical current but lower T_C [16]. Liao *et. al.* found that through a slow cooling process, the oxygen in bulk MgB_2 can segregate to form nanometer-sized coherent Mg(B,O) in the MgB_2 matrix acting as effective flux pinning centers without decreasing T_C [11]. Klie *et. al.* previously reported oxygen precipitates in bulk MgB_2, where oxygen was incorporated every second boron plane of the MgB_2 structure, found by atomic resolution electron energy loss spectroscopy (EELS) studies using a scanning transmission electron microscope [1]. Figure 1 shows an atomic resolution Z-contrast image of one of these oxygen precipitates taken from bulk MgB_2 along the [100] orientation. The increase of contrast every second column in Fig. 1 is due to the presence of oxygen [17]. The size of these precipitates was reported to be about 20-100 nm [1].

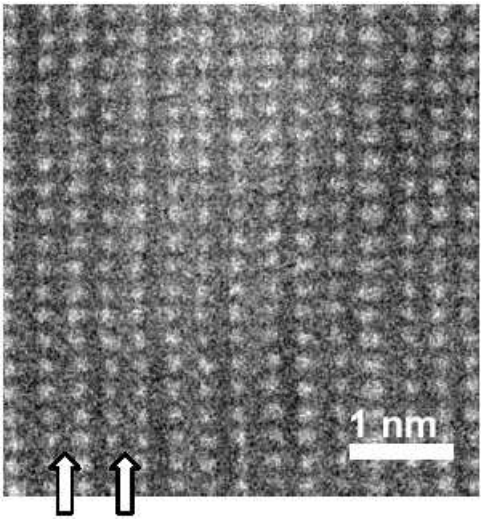


FIG. 1: Z-contrast image of a coherent oxygen precipitate in the bulk of MgB_2 [010]. The bright spots are Mg atoms. The increase of contrast every second column is due to presence of oxygen every second boron plane. White arrows highlight the atomic columns where oxygen has precipitated.

Motivated by these experimental observations, in this work we discuss the effects of oxygen-ordering, with different stoichiometries, on the electronic structure and superconductivity properties of MgB_2 via first-principles calculations. As possible candidates for the atomic structures of coherent oxygen precipitates in bulk MgB_2, we propose two different structures of composition, Mg_2B_3O and $Mg_2B_3O_2$. We find that incorporation of oxygen in the form of $Mg_2B_3O_x$ structures decreases the DOS at the Fermi energy and the electron phonon coupling compared with MgB_2. From total energy calculations we find that Mg_2B_3O is less stable compared to $Mg_2B_3O_2$ but has a higher T_C. It is important to notice that our calculations show that oxygen impurities are likely to be present everywhere in MgB_2 structures. Therefore, controlling the density and type of these impurities will finally be the limiting factor in improving the transport properties of MgB_2.

Our atomic and electronic structure calculations were performed using the ab initio pseudopotential plane wave method [18] within the generalized gradient approximation (GGA) [19], and local density approximation (LDA) for comparison. In order to compare the changes due to oxygen in MgB_2, we doubled the unit cell of MgB_2 in the c-direction. Brillouin-zone integrations were carried out with 15×15×6 Monkhorst-Pack grids for Mg_2B_4 and $Mg_2B_3O_x$. An energy cutoff of 400 eV was used for all the calculations. The lattice volumes, shapes, and all atoms were allowed to relax for the new structures using a force criterion of 10^{-2} eV/Å. The zone-center phonons and electron phonon couplings were calculated using density functional perturbation theory [20].

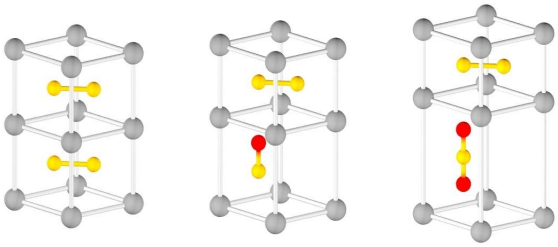


FIG. 2: (color). From left to right: schematics of Mg_2B_4, Mg_2B_3O and $Mg_2B_3O_2$ crystal structures. The lattice in the c-direction stretches for $Mg_2B_3O_2$ structures with respect to Mg_2B_4, where the addition of oxygen increases the distance between the Mg planes where oxygen was added. Mg, B, and O atoms are shown in gray, yellow, and red respectively.

The relaxed geometries for structures with partial substitution of boron atoms with one and two oxygen atoms, Mg_2B_3O and $Mg_2B_3O_2$, as well as Mg_2B_4, are shown in Fig. 2. Other oxygen concentrations were tried as well (i.e. $Mg_2B_3O_3$, where one additional oxygen was inserted in the boron plane), but these resulted in a significant distortion of the MgB_2-like symmetry and did not reproduce features observed in the coherent oxygen precipitates. We found that the incorporation of oxygen changes the well-defined B-B planes by the formation of BO_x units in the $Mg_2B_3O_x$ structures. Both $Mg_2B_3O_x$ structures belong to the space group P3m1 (C^1_{3v}, No. 156). The relevant structural parameters for the three structures considered are shown in Table I. Introduction of oxygen considerably increases the distance between neighboring Mg planes, but decreases the distance between the other Mg planes, which are above and below the boron layer left intact. As a result, the lattice stretches in the c-direction compared to Mg_2B_4. Such behavior was reported by Eom *et. al.* where thin films rich in oxygen showed a higher c lattice parameter suggesting that boron can be substituted by oxygen [16]. The calculated ratios of the distances between the Mg-BO_x-Mg and Mg-BB-Mg layers are 1.22 and 1.49 for the theoretical Mg_2B_3O and $Mg_2B_3O_2$ structures, respectively, while the estimate from the experimental image is 1.14 ± 0.05. The overestimated theoretical values for the ratios compared with the experimental can be explained in two different ways: (i) pressure effects from the surrounding bulk into the precipitate, which shrinks the lattice parameter in the c-direction, and (ii) the concentration of oxygen in the BO_x planes is slightly lower than the ones calculated here, where $x < 1$.

We also investigated the phase stability of the $Mg_2B_3O_x$ compounds relative to atomic constituents and bulk MgB_2. Both $Mg_2B_3O_x$ structures are stable against phase separation into their atomic constitutes. However, the magnitudes of the binding energies per atom for Mg_2B_3O are found to be 0.16 eV and 0.63 eV smaller compared to that of MgB_2 calculated using atomic oxy-

TABLE I: Summary of properties for MgB_2, Mg_2B_4, Mg_2B_3O and $Mg_2B_3O_2$ crystal structures. The $Mg_2B_3O_x$ structures belong to the space group P3m1 (C^1_{3v}, No. 156). Lattice parameters are in Å, $N(E_F)$ in states/eV, frequencies (ω) in meV. The parenthesis next to the frequencies indicates degeneracy of those modes. T_C is given in K. The lattice parameters are shown for GGA (LDA) approximations. The phonon modes, electron phonon coupling, and the critical temperatures were all calculated using the values from the GGA calculations.

MgB_2		Mg_2B_4		Mg_2B_3O		$Mg_2B_3O_2$	
a=3.086[a]		a=3.046(3.086)		a=3.067(3.016)		a=3.143(3.016)	
c=3.524[a]		c=7.054(7.048)		c=7.701(7.545)		c=8.633(8.231)	
$N(E_F)$=0.69[b]		$N(E_F)$=1.35(1.38)		$N(E_F)$=0.85(0.87)		$N(E_F)$=1.05(1.99)	
ω_p[b]	λ_p[b]	ω_p	λ_p	ω_p	λ_p	ω_p	λ_p
87.1(1)B_{1g}	-	26.3(2)	0	22.5(2)	0.027	10.0(2)	0.047
74.5(2)E_{2g}	0.907	27.0(2)	0.06	28.4(2)	0.029	16.8(2)	0.074
49.8(1)A_{2u}	-	39.0(1)	0.08	39.2(1)	0.109	21.0(2)	0
40.7(1)E_{1u}	-	39.7(2)E_{1u}	0	39.3(2)	0.010	25.0(2)	0.003
		47.6(1)	0	48.9(2)	0.026	33.6(1)	0
		49.3(1)A_{2u}	0	51.0(1)	0.019	36.5(1)	0.124
		68.0(2)	0.51	53.0(1)	0.005	41.2(2)	0.002
		73.4(2)E_{2g}	0.46	72.1(2)	0.506	55.4(1)	0
		79.2(1)	0.03	90.4(1)	0.002	83.1(1)	0
		86.3(1)B_{1g}	0	161.8(1)	0.088 5	89.121)	0.153
						105.3(1)	0.131
						215.8(1)	0
$\lambda = 0.907$		$\lambda = 1.14$		$\lambda = 0.821$		$\lambda = 0.534$	
$\omega_{log} = 74.5$		$\omega_{log} = 64.5$		$\omega_{log} = 65.6$		$\omega_{log} = 48.9$	
$T_C = 39.4$		$T_C = 40.73$		$T_C = 18.31$		$T_C = 1.62$	

[a]Taken from Ref. [2]
[b]Values for $N(E_F)$, ω, λ and T_C (with $\mu^* = 0.15$) are taken from Ref. [26]

gen, and molecular oxygen, respectively. On the other hand, the magnitudes of the binding energies per atom for $Mg_2B_3O_2$ are 0.11 eV higher, and 0.71 eV lower compared to that of MgB_2 calculated using atomic oxygen, and molecular oxygen, respectively. These calculations suggest that (i) the theoretical $Mg_2B_3O_x$ structures are not stable against phase separation into MgB_2 and molecular oxygen, and (ii) $Mg_2B_3O_2$ is stable with respect to phase separation into MgB_2 and atomic oxygen. This does not, however, mean that these structures have to be ruled out as possible candidates for coherent oxygen precipitates, since they can still exist as metastable phases in bulk MgB_2.

Figure 3 shows the calculated unoccupied boron DOS for the theoretical $Mg_2B_3O_x$ nanostructures compared with the experimental boron K-edge spectra taken from the B-B plane (darker columns in Fig. 1) and BO_x plane (brighter columns in Fig. 1) respectively. Each experimental spectrum is the sum of seven individual spectra with an acquisition time of 1 sec. and an energy resolution of 1.2 eV. The spectra have been summed up to increase the signal to noise ratio, and background subtracted and corrected for multiple-scattering contributions [1]. To obtain a better comparison between theory

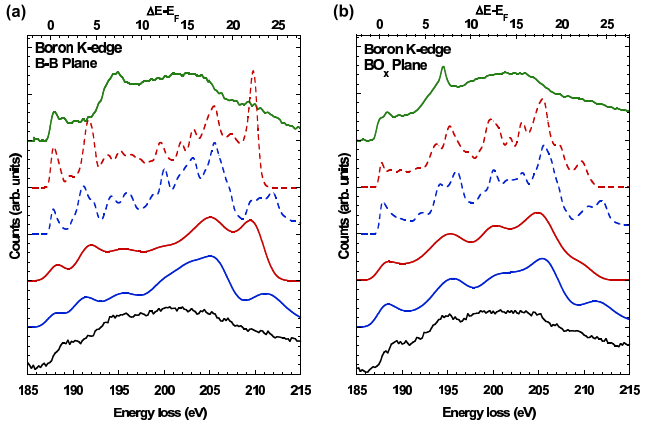


FIG. 3: (color). Experimental Boron K-edge spectra of coherent oxygen precipitate (black) compared with calculated density of states of Mg_2B_3O (blue) and $Mg_2B_3O_2$ (red) (a) B-B plane, and (b) BO_x plane. Solid (dashed) lines have an energy resolution of 1.2 (0.4) eV. Experimental monochromated spectra (green) with an energy resolution of 0.3 eV are shown for comparison for (a) bulk MgB_2, and (b) a precipitate region with oxygen. Notice that the pre-peak in the Boron K-edge is completely resolved for (a) and (b). Changes due to oxygen in the monocromated spectra (b) are clearly notorious, change of intensity in the pre-peak and the peak at 195 eV.

and experiment, we have calculated the boron p_{xy} and p_z states. We then took into account the scattering momentum transfer dependence of the electron microscope optical conditions and crystal orientation to weigh the boron p_{xy} and p_z states according to the experimental setup [21]. Analysis of the spectra for energies in the range of 15-20 eV above the Fermi level was not performed, since multiple scattering and lifetime broadening limit the resolution of the spectra, which makes comparison between experiment and theory uncertain in that regime [21]. The theoretical spectra was obtained in the Z approximation, which has worked well for bulk MgB_2 [21], have been convoluted for an energy resolution of 1.2 eV and 0.4 eV (shown for comparison purposes only). Figure 3(a) shows the experimental and theoretical spectra for the B-B plane, where both structures, Mg_2B_3O and $Mg_2B_3O_2$ (energy resolution of 1.2 eV), have good agreement with experiment. The pre-peak of the boron K-edge at 189 eV in the experiment is well reproduced in both theoretical structures. A peak at 192 eV, which is present in both theoretical spectra, is not resolved in the experimental spectra. This is possibly due to the low signal to noise ratio of the experimental spectra. Figure 3(b) shows the spectra for the BO_x plane, where the enhancement of the peak at 195 eV, which was previously attributed to oxygen [1, 11, 22], is very well predicted by both theoretical structures. This peak has a lower intensity for the B-B plane spectra (Fig. 3(a)). Finally, the pre-peak in the BO_x plane experimental spectra shows an enhancement in intensity compared with the B-B plane experimental spectra. Here, both theoretical spectra present a remarkable agreement with the experiment, especially the Mg_2B_3O structure where the difference in intensity of the pre-peak between the B-B plane and the BO_x plane spectra is more pronounced. Additionally, monochromated spectra (energy resolution of 0.3 eV) from bulk MgB_2 and a region containing oxygen are shown in Fig. 3(a) and Fig. 3(b), respectively. Notice that the pre-peak is completely resolved for Fig. 3(a) and Fig. 3(b). Furthermore, the monochromated spectrum (Fig. 3(b)) presents an enhancement due to oxygen of the peak at 195 eV.

To investigate the effect of oxygen incorporation by partial boron substitution on the superconducting properties of MgB_2, we first calculated the phonon modes and electron phonon coupling parameters for Mg_2B_4, Mg_2B_3O, and $Mg_2B_3O_2$. The results are shown in Table I. In order to obtain the transition temperatures T_C of the theoretical $Mg_2B_3O_x$ nanostructures we used the McMillian expression [23]

$$T_C = \frac{\omega_{log}}{1.2} \exp\left(\frac{-1.04(1+\lambda)}{\lambda - \mu^*(1+0.62\mu^*\lambda)}\right), \qquad (1)$$

where ω_{log} is the logarithmic average frequency, λ is the total electron phonon coupling defined as $\lambda = \sum_{p\in\Gamma} \lambda_p$, with λ_p being the electron phonon coupling for each mode at Γ, and μ^* represents the Coulomb repulsion interaction. We used the value of $\mu^* = 0.19$. In the case of MgB_2, the Eliashberg function has a sharp peak around the E_{2g} mode [24]; therefore, it is sufficient to take the E_{2g} mode energy as ω_{log} to obtain the transition temperature T_C [25, 26]. In fact, using only this mode, not only T_C but also the isotope effect and pressure dependence of T_C can be successfully explained [27]. However, for the $Mg_2B_3O_x$ nanostructures, the E_{2g} mode is no longer well defined and ω_{log} has to be averaged throughout all the phonon modes. We approximated ω_{log} as $\omega_{log} \approx \exp\left(\frac{1}{\lambda}\sum_n \ln(\omega_p)\lambda_p\right)$, and only calculated the phonons at the zone center Γ. We obtained transition temperatures T_C of 40.73 K, 18.31 K, and 1.62 K for Mg_2B_4, Mg_2B_3O, and $Mg_2B_3O_2$, respectively.

In conclusion, we have proposed two different structures, Mg_2B_3O and $Mg_2B_3O_2$ as possible candidates for the $Mg_2B_3O_x$ nanostructures observed experimentally in bulk MgB_2 [1]. Both structures present an increase of the c lattice parameter with respect to Mg_2B_4, where the Mg_2B_3O structure is closer to the experimental value. The experimental spectra for the B-B plane and BO_x plane are well explained by the Mg_2B_3O and $Mg_2B_3O_2$ structures. Both structures are good candidates for coherent oxygen precipitates, although their superconductivity properties differ. $Mg_2B_3O_2$ precipitates would behave as a pinning center for temperatures higher than 2 K, while Mg_2B_3O precipitates would start to behave as a pinning center for temperatures higher than 18 K. Our results show that oxygen impurities are likely to be present everywhere in MgB_2, highlighting the importance of oxygen as an agent in the creation of flux pinning centers and as a factor of improvement upon the critical current density J_C.

J. C. Idrobo thanks H. J. Choi for useful discussions and R. Erni for assistance on the FEI G2 Tecnai electron microscope. This work was supported by DOE, NSF, and LBNL.

* Electronic address: jidrobo@lbl.gov

[1] R. F. Klie, J. C. Idrobo, N. D. Browning, A. Serquis, Y. T. Zhu, X. Z. Liao, and F. M. Mueller, Appl. Phys. Lett. **80**, 3970 (2002).
[2] J. Nagamasu, N. Nakagawa, T. Muranaka, Y. Zenitani, and J. Akimitsu, Nature **410**, 63 (2001).
[3] J. Wang, Y. Bugoslavsky, B. Berenov, L. Cowey, A. D. Caplin, L. F. Cohen, L. D. Cooley, X. Song, and D. C. Larbalestier, Appl. Phys. Lett. **81**, 2026 (2002).
[4] Y. Feng *et. al.*, Appl.Phys. Lett. **79**, 3983 (2001).
[5] T. Takenobu, T. Ito, D. H. Chi, et. al., Phys. Rev. B **64**, 134513 (2001).
[6] J.S Slusky, *et. al.* Nature **410**, 343 (2001).
[7] S. Soltanian, X. L. Wang, J. Hovart, *et. al.* Physica C

382, 187 (2002).
[8] Y. Yan and M. M. Al-Jassim., Phys. Rev. B **67**, 212503 (2003).
[9] P. A. Sharma, N. Hur, Y. Horibe, C. H. Chen, B. G. Kim, S. Guha, M. Z. Cieplak, and S-W. Cheong, Phys. Rev. Lett. **89**, 167003 (2002).
[10] R. F. Klie, J. C. Idrobo, N. D. Browning, K. A. Regan, N. S. Rogado, and R. J. Cava, Appl. Phys. Lett. **79**, 1837 (2001).
[11] X. Z. Liao, A. Serquis, Y. T. Zhu, J. Y. Huang, L. Civale, D. E. Peterson, F. M. Mueller, and H. F. Xu, Journal of Appl. Phys. **93**, 6208 (2003).
[12] D. Larbalestier, A. Gurevich, M. Feldmann, and A. Polyanskii, Nature **414**, 368 (2001).
[13] P. C. Canfield, D. K. Finnemore, S. L. Budko, J. E. Ostenson, G. Lapertot, C. E. Cunningham, and C. Petrovic, Phys. Rev. Lett. **86**, 2423 (2001).
[14] Grasso *et. al.* Appl. Phys. Lett. **79**, 230 (2001).
[15] D. Mijatovic, A. Brinkman, I. Oomen, G. Rijnders,H. Hilgenkamp, H. Rogalla, and D. H. A. Blank, Appl. Phys. Lett. **80**, 2141 (2002).
[16] C. B. Eom, M. K. Lee, J. H. Choi, L. J. Belenky, X. Song, L. D. Cooley, M. T. Naus, S. Patnaik, J. Jiang, M. Rikel, A. Polyanskii, A. Gurevich, X. Y. Cai, S. D. Bu, S. E. Babcock, E. E. Hellstrom, D. C. Larbalestier, N. Rogado, K. A. Regan, M. A. Hayward, T. He, J. S. Slusky, K. Inumaru, M. K. Haas, and R. J. Cava, Nature **411**, 588 (2001).
[17] For further information in the experimental techniques see N. D. Browning, M. F. Chisholm, and S. J. Pennycook, Nature **366**, 143 (1993).
[18] G. Kresse and J. Furthmuller, Phys. Rev. B **54**, 11169 (1996).
[19] J. P. Perdew, J. A. Chevary, S. H. Vosko, K. A. Jackson, M. R. Pederson, D. J. Singh, and C. Fiolhais, Phys. Rev. B **46**, 6671 (1992).
[20] S. Baroni, S. Gironcoli, A. Dal Corso, and P. Giannozzi, Rev. Mod. Phys. **73**, 515 (2001).
[21] R. F. Klie, H. Su, Y. Zhu, J. Davenport, J. C. Idrobo, N. D. Browning, and P. D. Nellist, Phys. Rev. B **67**, 144508 (2003).
[22] Y. Zhu, A. R. Moodenbaugh, G. Schneider, J. W. Davenport, T. Vogt, Q. Li, G. Gu, D. A. Fisher, J. Tafto, Phys. Rev. Lett. **88**, 247002 (2002).
[23] W. L. McMillan, Phys. Rev. **167**, 331 (1968).
[24] H. J. Choi, D. Roundy, H. Sun, M. L. Cohen, and S. G. Louie, Nature **418**, 758 (2002); J. Choi, M. L. Cohen, and S. G. Louie Physica C **385**, 66 (2003).
[25] J. M. An and W. E. Pickett, Phys. Rev. Lett. **86**, 4366 (2001).
[26] T. Yildirim, O. Gulseren, J. W. Lynn, C. M. Brown, T. J. Udovic, Q. huang, N. Rogado, K. A. Regan, M. A. Hayward, J. S. Slusky, T. He, M. K. Haas, P. Khalifah, K. Inamaru, and R. J. Cava, Phys. Rev. Lett. **87**, 037001 (2001).
[27] T. Yildirim and O. Gulseren, J. Phys. Chem. Solids **63**, 2201 (2002)